H-shaped terahertz patch antenna with metamaterials for biomedical applications

Kaoutar Saidi Alaoui¹, Siraj Younes², Foshi Jaouad²

¹EST Dakhla, Ibn Zohr University, Dakhla, Morocco

²ERTTI Laboratory, Faculty of Science and Technology FST Errachidia, Moulay Smail University, Errachidia, Morocco

Article Info

Article history:

Received Nov 6, 2024 Revised Jul 29, 2025 Accepted Sep 16, 2025

Keywords:

Antenna impedance matching Biomedical Metamaterials Patch antenna Terahertz

ABSTRACT

This paper presents the design and simulation of an H-shaped terahertz microstrip patch antenna integrated with a metamaterial (MTM) layer to enhance performance for biomedical sensing applications. The antenna modeled using high frequency structure simulator (HFSS), is optimized for 4.37 THz operation. While FR4 is used in simulations for baseline analysis, alternative low-loss substrates such as polyimide or quartz are recommended for practical THz applications. The antenna design uses an FR4 substrate with a dielectric constant of 4.4 and a thickness of 2 μ m. Ground plane, feed line, and patch are made of copper material. The integration of the MTM enhance clearly the antenna characteristics. This integration helps to improve the antenna impedance matching; the reflection coefficients was enhanced from -25.01 to -63.10 dB. Additionally, this integration boost also the antenna radiation characteristics, increasing the gain from 2.62 to 3.86 dB and the directivity from 3.57 to 4.97 dB.

This is an open access article under the CC BY-SA license.



5215

Corresponding Author:

Kaoutar Saidi Alaoui EST Dakhla, Ibn Zohr University Dakhla, Morocco

Email: k.alaouisaidi@uiz.ac.ma

1. INTRODUCTION

Terahertz (THz) waves refer to electromagnetic radiation with frequencies ranging from 0.1 to 10 THz (wavelengths between 30 and 3,000 μm), sitting between the microwave and infrared regions of the spectrum. Compared to other frequency bands, THz waves exhibit strong penetration through many non-polar and non-metallic materials but are heavily absorbed by water molecules. Due to their low photon energy, THz radiation is non-ionizing and non-invasive. Organic molecules often display strong absorption and scattering in the THz range because of the low-frequency vibrational and rotational transitions unique to each molecule, creating characteristic "fingerprint spectra" [1]–[3]. As a result, THz technology finds applications in fields like food science, agriculture, biology, security screening and communications [4]–[13].

Designing efficient THz antennas presents significant challenges due to intrinsic properties of THz waves, like limited penetration depth and high propagation losses. Addressing these issues requires innovative techniques to improve antenna performance. Several solutions have been proposed, including slotting techniques [14], alternative substrates [15], partial ground planes [16], [17], and meta-surfaces [18], with the most promising approach being the use of metamaterials [19].

Metamaterials are synthetic structures specifically designed to possess electromagnetic characteristics that do not exist in naturally occurring materials [20]. Through the precise tuning of their permittivity and permeability, these materials enable exceptional control over electromagnetic wave behavior, which can substantially enhance the performance of devices like terahertz (THz) antennas [21].

5216 □ ISSN: 2088-8708

This work focuses on the performance optimization of terahertz (THz) H-shaped patch antennas through the incorporation of specifically engineered metamaterial structures, aiming to fulfill stringent requirements associated with biomedical sensing and imaging applications. A novel metamaterial unit cell, designed for efficient operation in the THz frequency band, is proposed to address persistent challenges such as limited operational bandwidth, suboptimal radiation efficiency, and impedance mismatching. The study encompasses full-wave electromagnetic simulations and rigorous theoretical modeling to quantify the impact of the metamaterial on key antenna performance indicators, including radiation efficiency, gain, and directivity. Additionally, a comprehensive analysis of the electromagnetic interaction mechanisms is conducted, emphasizing the influence of the metamaterial on wave propagation dynamics, resonance behavior, and impedance transformation characteristics within the THz regime.

The structure of the paper is as follows: section 1 details the design methodologies and physical configurations of both the H-shaped antenna and the metamaterial inclusion. Section 2 presents a thorough discussion of the numerical results supported by analytical validation. The final section synthesizes the main findings, outlines the study's limitations, and proposes future research directions to further exploit metamaterial-enabled enhancements in THz antenna systems.

2. METHOD

2.1. The configuration of the antenna

The proposed design uses FR4 as the substrate with a thickness of 2 μ m and dielectric constant ε_r =4.4. While FR4 is widely adopted in microwave applications, its use at terahertz frequencies is limited due to its high dielectric losses and mechanical fragility at small thicknesses. It is selected here only for simulation purposes. In practical THz implementations, low-loss substrates such as quartz, polyimide, or high-resistivity silicon are preferred.

The metallic components (patch, feed line, and ground) are modeled using copper with a conductivity of 5.8×10^7 S/m and a thickness of $0.5~\mu m$, which exceeds the skin depth at 4.37 THz. This ensures proper current conduction despite high-frequency losses. Alternative materials such as gold or silver could further reduce ohmic losses.

Our antenna features a patch design with a partial ground structure, implemented on an FR4 substrate, measuring L×W in total dimensions. The measurements of the patch antenna were established utilizing the subsequent equations [22]:

$$W_p = \frac{c}{2f} \sqrt{\frac{2}{\varepsilon_r + 1}} \tag{1}$$

where C is the velocity of light, f the frequency and ε_r is the dielectric of the substrate.

$$\varepsilon_{\text{reff}} = \frac{\varepsilon_r + 1}{2} + \frac{\varepsilon_r - 1}{2} \left[1 + \frac{12h}{w} \right]^{\frac{1}{2}} \tag{2}$$

where ε_{ref} is the effective dielectric and h_s the substrate thickness,

$$\Delta L = 0.412 h_s \frac{(\epsilon_{ref} + 0.3) \left(\frac{w}{h_s} + 0.264\right)}{(\epsilon_{ref} - 0.258) \left(\frac{w}{h_s} + 0.8\right)}$$
(3)

where ΔL is the length extension.,

$$Lp = L_{eff} - 2 \triangle L \tag{4}$$

where Lp is the patch length and L_{eff} is the effective length.

$$L_{eff} = \frac{c}{2f_r \sqrt{\varepsilon_{reff}}} \tag{5}$$

2.2. The antenna design

The H-shaped patch antenna is a variant of the traditional rectangular patch antenna but with an "H"-like geometry that offers several performance advantages. The horizontal and vertical segments of the H-shaped patch can be optimized to achieve desired resonant frequencies, bandwidth, and polarization

characteristics. This design inherently supports multi-band operations due to the presence of multiple resonant modes, making it ideal for broadband applications such as biomedical. For the proposed design, the antenna's radiating element is fabricated on an FR4 substrate with a relative dielectric constant (ε_r = 4.4), a loss tangent of 0.02, and a physical thickness of 2 µm, ensuring mechanical stability and consistent electromagnetic behavior within the designated frequency range. The proposed antenna, is created by cutting two parallel slots into a rectangular patch. This structure allows for better control of the antenna's resonant frequency and bandwidth, enabling improved performance compared to a standard rectangular patch. The slots within the patch help in fine-tuning the impedance matching and achieving dual or wide-band operation. These slots can also reduce the physical size of the antenna while maintaining its electrical length, making the antenna more compact. Figure 1 offers a detailed view of the antenna's structure and illustrates the iterative design process used. Table 1 outlines the key physical dimensions of the proposed antenna, which were optimized to ensure proper resonance and impedance matching within the targeted THz frequency range.

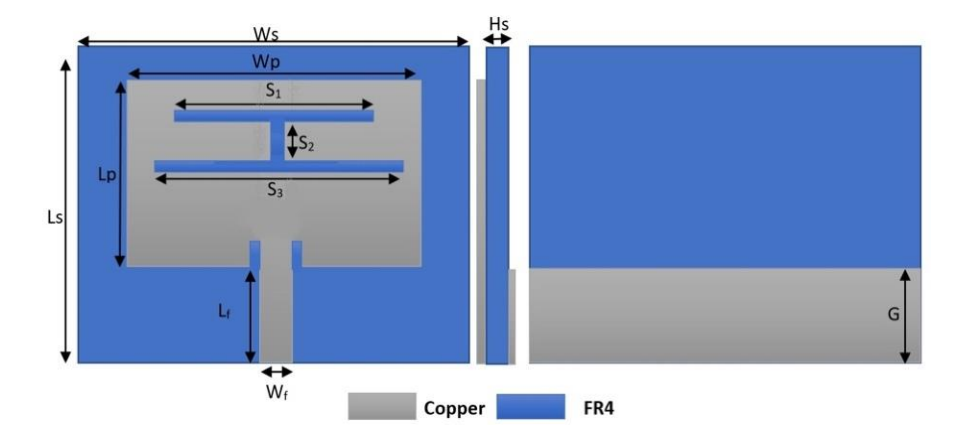


Figure 1. The proposed H-shaped patch antenna design

T	Table 1. Antenna dimensions			
Variable	Value (µm)	Variable	Value (µm)	
W_{s}	69	g	15	
L_{s}	54	Wf	4.8	
L_{pa}	34	Lf	15	
W_{pa}	52	S_1	30	
hs	2	S_2	10	
		S_2	38	

2.3. The metamaterials design

The designed metamaterial (MTM) structure consists of a 3×3 array of unit cells, occupying a total area of $W_M\times L_M$, and implemented on an FR4 substrate with a thickness of 2 μm . Each unit cell is composed of a split-ring resonator (SRR), formed by two concentric metallic rings with a defined gap C of 2 μm , enabling resonance at THz frequencies. The geometric configuration and topology of the SRR elements are depicted in Figure 2. The detailed dimensional specifications, including both the overall MTM array and individual SRR unit cell parameters, are provided in Table 2. The metamaterial layer is strategically placed at a vertical distance of 20 μm beneath the radiating antenna structure to maximize electromagnetic coupling and enhance radiation performance. The MTM layer is assumed to be supported by a thin dielectric layer, ensuring structural feasibility and maintaining consistent electromagnetic coupling. The simulation setup avoids suspension in air and considers a realistic integration scenario.

The MTM layer is positioned at a vertical offset of 20 µm beneath the radiating patch. This spatial configuration plays a crucial role in enhancing the antenna's overall electromagnetic performance, particularly by improving impedance matching and radiation efficiency. The intentional placement of the MTM contributes to the suppression of reflected waves and mitigates undesired back radiation, resulting in improved forward energy transmission and reduced power losses. The relative positioning of the MTM structure with respect to the antenna is illustrated in Figures 3(a) and 3(b).

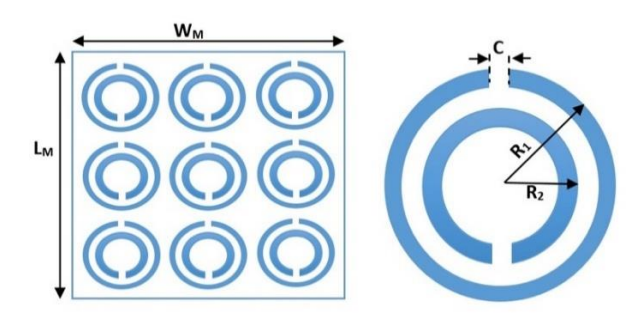


Figure 2. Design methodology of the proposed metamaterial layout and unit cell geometry

Table 2. MTM dimensions			
Variable	Value(µm)	Variable	Value(µm)
W_{M}	79	R2	6
L_{M}	66	C	2
R1	10		

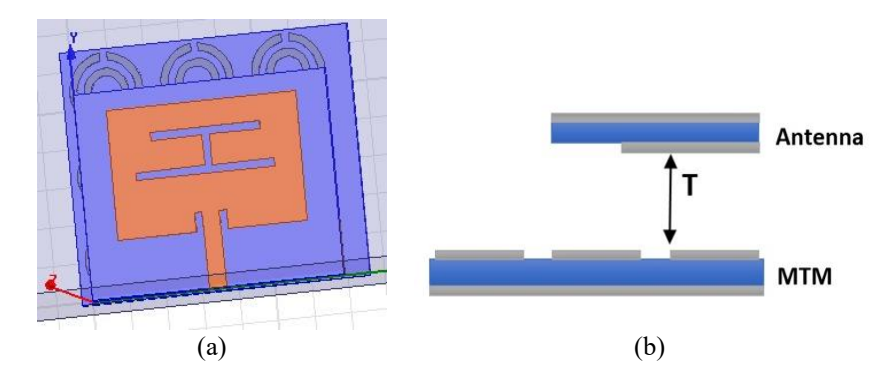


Figure 3. The proposed MTM based antenna architecture (a) top view and (b) side view

3. RESULTS AND DISCUSSION

3.1. Reflection coefficient and VSWR

Figure 4 illustrates the reflection coefficient (S11) and voltage standing wave ratio (VSWR) of the proposed antenna, both with and without the MTM. The inclusion of the MTM results in a substantial improvement in antenna performance, as evidenced by a significant reduction in S11 from -25.01 to -63.10 dB. This indicates much better impedance matching and a considerable decrease in the reflection of incident electromagnetic waves, which enhances the efficiency of the antenna.

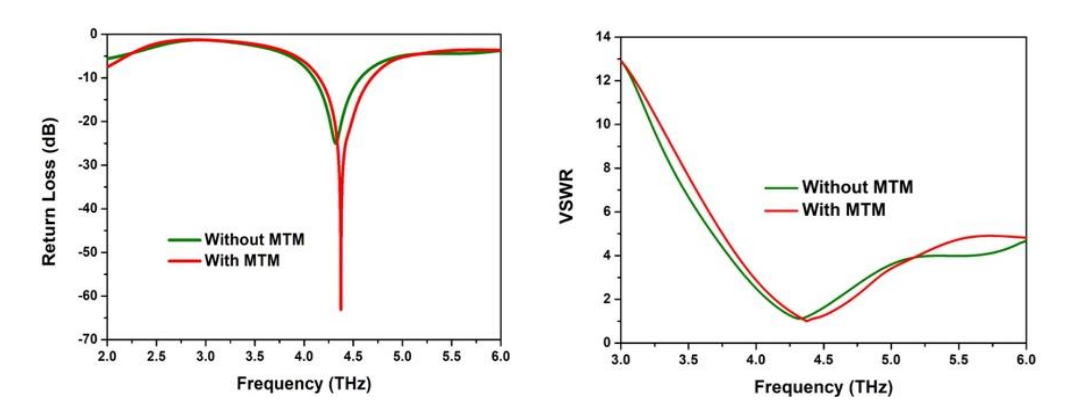


Figure 4. Reflection coefficient and VSWR of the proposed antenna with and without MTM

In addition to the improvement in S11, the VSWR is also significantly enhanced, dropping from 1.118 to 1.001. This near-ideal VSWR value demonstrates almost perfect impedance matching, which minimizes energy loss and ensures efficient transmission of electromagnetic energy through the antenna. These improvements highlight the critical role of the MTM in optimizing the antenna's overall performance.

3.2. Gain

The radiation pattern of an antenna is a key indicator of how efficiently electromagnetic energy is radiated into space. Figures 5(a) and 5(b) illustrate the 2D radiation patterns without and with the MTM, while Figures 5(c) and 5(d) present the corresponding 3D representations. A clear improvement in gain is observed with the integration of the MTM, increasing from 2.62 to 3.86 dB. This confirms the MTM's effectiveness in enhancing the antenna's performance. By introducing the MTM structure, the radiation pattern becomes more focused, with reduced side lobes and a stronger main lobe, improving directionality and overall radiation efficiency. Placed beneath the substrate, the MTM modifies the near-field distribution by constructively redirecting surface currents toward the broadside direction. This not only confines the radiated energy more effectively but also minimizes undesired radiation. Additionally, the MTM contributes to polarization stability by aligning the dominant current paths along the feed axis.

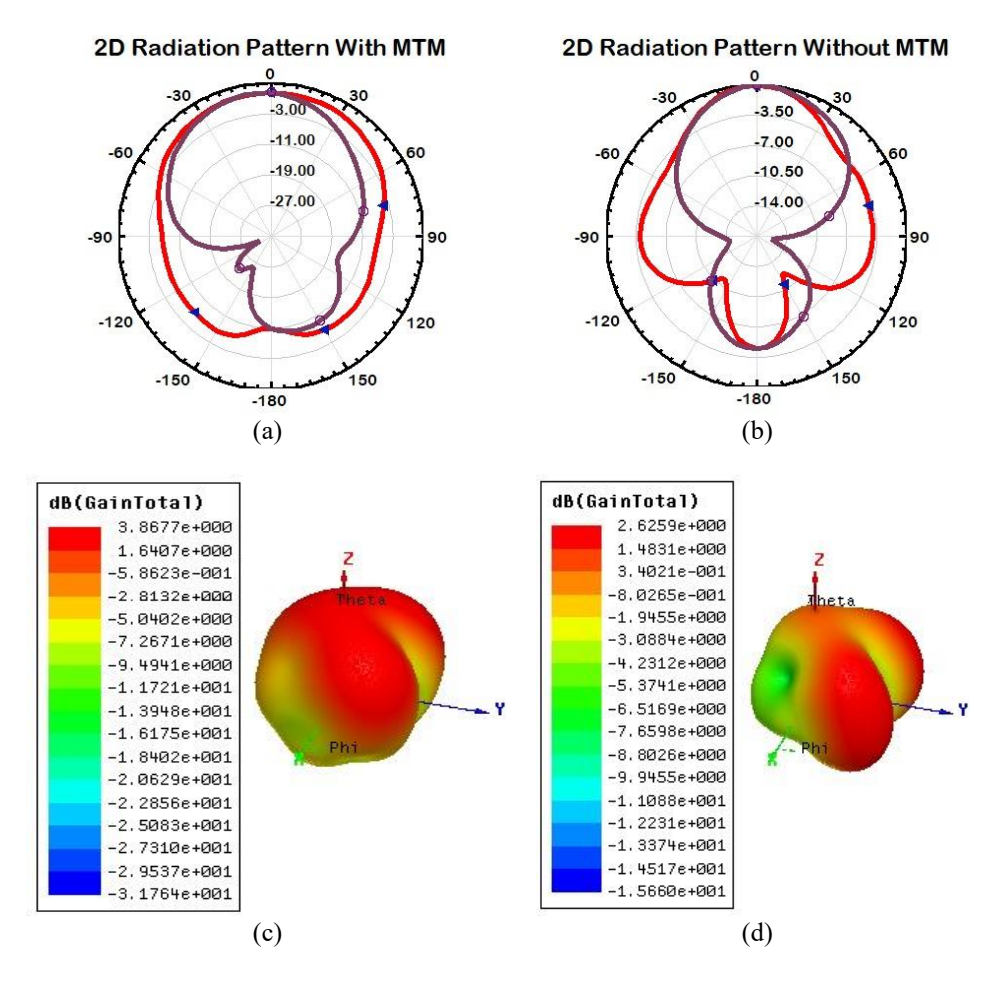


Figure 5. Gain of the proposed antenna (a) 2D with MTM, (b) 2D without MTM, (c) 3D with MTM, and (d) 3D without MTM

3.3. Directivity

Figure 6 presents the simulated directivity patterns of the proposed antenna in two configurations: Figure 6(a) with the integrated MTM layer and Figure 6(b) without it. The incorporation of the MTM results in a substantial enhancement in directivity, increasing from 3.57 to 4.97 dB corresponding to an approximate improvement of 39.21%. This considerable gain highlights the MTM's effectiveness in improving the antenna's directional radiation characteristics by concentrating the radiated energy more efficiently along the main beam axis. By acting as a reflector, the MTM helps to reduce undesired radiation in other directions,

5220 SISSN: 2088-8708

ensuring that more of the transmitted energy is concentrated in the intended direction. This not only improves the antenna's directional performance but also contributes to overall system efficiency, making the antenna more effective for biomedical applications.

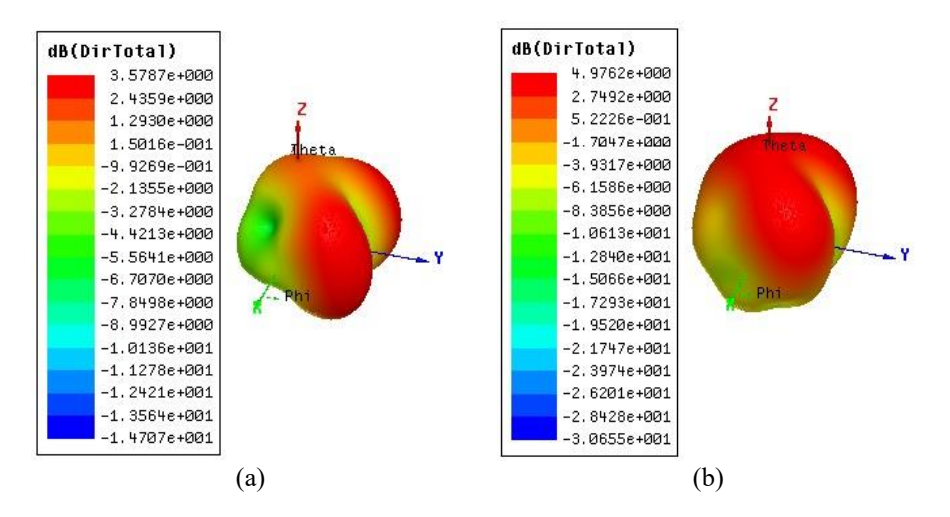


Figure 6. Directivity of the proposed antenna (a) with MTM and (b) without MTM

The observed end-fire radiation pattern in the base structure is attributed to asymmetry in the partial ground plane and substrate effects at THz frequencies. While patch antennas typically radiate in the broadside direction, miniaturized and high-frequency effects can distort this behavior. With MTM integration, a more stable broadside response is recovered. Table 3 highlights the impact of MTM integration on key antenna characteristics by contrasting the results obtained with and without the metamaterial structure.

Table 3. Antenna performance comparison with and without MTM

	Without MTM	WITH MTM
S ₁₁ (dB)	-25.01	-63.10
VSWR	1.118	1.001
Gain (dB)	2.62	3.86
Directivity (dB)	3.57	4.97

The Table 4 compares different antenna designs based on size, operating frequency, S11 (reflection coefficient), and gain. The antennas in references [14], [23]–[25] have sizes ranging from $23\times19~\mu\text{m}^2$ to $50\times50~\mu\text{m}^2$, with frequencies between 4.60 and 4.95 THz. These designs achieve S11 values between -38.00 and -55.31 dB, indicating good impedance matching, and their gain varies from 3.10 to 5.06 dB.

Table 4. Antenna performance comparison with other antenna designs

Ref.	Size (µm²)	Frequency (THz)	S ₁₁ (dB)	Gain (dB)
[23]	23×19	4.95	-55.31	4.25
[24]	32×36	4.60	-44.28	3.10
[14]	50×50	4.83	-38.00	4.30
[25]	49×35	4.92	-44.73	5.06
This work	69×54	4.37	-63.10	3.86

In contrast, the design in "this work" stands out with a significantly larger size of $69\times54~\mu m^2$ and a lower operating frequency of 4.37 THz. Despite the larger size, this design achieves the best S11 value of -63.10 dB, showing excellent impedance matching, far surpassing the other designs. Although its gain (3.86 dB) is slightly lower than some other designs, the superior S11 performance makes it highly efficient in reducing signal reflection, demonstrating the antenna's improved design and efficiency.

3.4. Efficiency

The Table 5 illustrates the radiation efficiency, calculated as gain/directivity, was found to be 73.1% without MTM and 77.7% with MTM, confirming the benefit of the metamaterial not only in directionality but also in reducing unwanted losses.

Table 5. Radiation efficiency

Configuration	Gain (dB)	Directivity (dB)	Efficiency (%)
Without MTM	2.62	3.57	73.1
With MTM	3.86	4.97	77.7

4. CONCLUSION

The combination of H-shaped terahertz patch antennas with metamaterials presents a significant leap forward in the development of high-performance antennas for biomedical applications. The proposed antenna employs a slotted radiating patch with a partial ground plane configuration, coupled with a MTM layer composed of a 3 × 3 array of SRR elements. The integration of the MTM structure leads to significant enhancements in the antenna's electromagnetic performance. Notably, the reflection coefficient (S₁₁) improves from -25.01 to -63.10 dB, the gain increases from 2.62 to 3.86 dB, and the directivity rises from 3.57 to 4.97 dB. These marked improvements underscore the synergistic effect of MTM integration, demonstrating its potential to significantly boost radiation efficiency and impedance matching. Consequently, the proposed design shows strong promise for high-performance applications, particularly in biomedical sensing and imaging domains. While the SRR unit cell geometry is conventional, the novelty of the present work lies in the optimized spatial integration of the MTM with the patch structure. This alignment enables effective resonance coupling, enhancing reflection suppression, gain, and directivity simultaneously in the THz band. For more experiments with the proposed design, the SAR calculation can be done in the future.

REFERENCES

- C. Rønne and S. R. Keiding, "Low frequency spectroscopy of liquid water using THz-time domain spectroscopy," *Journal of Molecular Liquids*, vol. 101, no. 1–3, pp. 199–218, Nov. 2002, doi: 10.1016/S0167-7322(02)00093-4.
- [2] E. Berry et al., "Do in vivo terahertz imaging systems comply with safety guidelines?," Journal of Laser Applications, vol. 15, no. 3, pp. 192–198, Aug. 2003, doi: 10.2351/1.1585079.
- [3] N. M. Burford and M. O. El-Shenawee, "Review of terahertz photoconductive antenna technology," *Optical Engineering*, vol. 56, no. 1, p. 10901, Jan. 2017, doi: 10.1117/1.OE.56.1.010901.
- [4] L. Afsah-Hejri, P. Hajeb, P. Ara, and R. J. Ehsani, "A comprehensive review on food applications of terahertz spectroscopy and imaging," *Comprehensive Reviews in Food Science and Food Safety*, vol. 18, no. 5, pp. 1563–1621, Sep. 2019, doi: 10.1111/1541-4337.12490.
- [5] C.-H. Feng and C. Otani, "Terahertz spectroscopy technology as an innovative technique for food: Current state-of-the-Art research advances," Critical Reviews in Food Science and Nutrition, vol. 61, no. 15, pp. 2523–2543, Aug. 2021, doi: 10.1080/10408398.2020.1779649.
- [6] L. Afsah-Hejri, E. Akbari, A. Toudeshki, T. Homayouni, A. Alizadeh, and R. Ehsani, "Terahertz spectroscopy and imaging: A review on agricultural applications," *Computers and Electronics in Agriculture*, vol. 177, p. 105628, Oct. 2020, doi: 10.1016/j.compag.2020.105628.
- [7] H. Ge et al., "Applications of THz spectral imaging in the detection of agricultural products," Photonics, vol. 8, no. 11, p. 518, Nov. 2021, doi: 10.3390/photonics8110518.
- [8] X. Yang et al., "Biomedical applications of terahertz spectroscopy and imaging," Trends in Biotechnology, vol. 34, no. 10, pp. 810–824, 2016, doi: 10.1016/j.tibtech.2016.04.008.
- [9] M. Wan, J. J. Healy, and J. T. Sheridan, "Terahertz phase imaging and biomedical applications," *Optics & Laser Technology*, vol. 122, p. 105859, Feb. 2020, doi: 10.1016/j.optlastec.2019.105859.
 [10] Z. Yan, L.-G. Zhu, K. Meng, W. Huang, and Q. Shi, "THz medical imaging: from in vitro to in vivo," *Trends in Biotechnology*,
- [10] Z. Yan, L.-G. Zhu, K. Meng, W. Huang, and Q. Shi, "THz medical imaging: from in vitro to in vivo," *Trends in Biotechnology*, vol. 40, no. 7, pp. 816–830, Jul. 2022, doi: 10.1016/j.tibtech.2021.12.002.
- [11] T. Li, L. Zhang, J. A. He, S. X. Zhang, and D. Y. Gu, "Terahertz time-domain spectroscopy for identification of hazardous substances in mail," *Guang Pu Xue Yu Guang Pu Fen Xi/Spectroscopy and Spectral Analysis*, vol. 39, no. 12, pp. 3724–3730, 2019, doi: 10.3964/j.issn.1000-0593(2019)12-3724-07.
- [12] A. Hirata and M. Yaita, "Ultrafast terahertz wireless communications," IEEE Transactions on Terahertz Science and Technology, vol. 5, no. 6, pp. 1128–1132, 2015.
- [13] W. Feng, S.-T. Wei, and J.-C. Cao, "6G technology development vision and terahertz communication," *Acta Physica Sinica*, vol. 70, no. 24, p. 244303, 2021, doi: 10.7498/aps.70.20211729.
- [14] S. M and G. M. M, "Performance predictions of slotted graphene patch antenna for multi-band operation in terahertz regime," Optik, vol. 204, p. 164223, Feb. 2020, doi: 10.1016/j.ijleo.2020.164223.
- [15] M. A. K. Khan, T. A. Shaem, and M. A. Alim, "Graphene patch antennas with different substrate shapes and materials," Optik, vol. 202, p. 163700, Feb. 2020, doi: 10.1016/j.ijleo.2019.163700.
- [16] F. Alam, M. A. Islam, M. F. Ahmed, M. M. Islam, and M. H. Kabir, "Design of elliptical patch antenna with partial ground at THz frequency band," in 2022 International Conference on Recent Progresses in Science, Engineering and Technology (ICRPSET), Dec. 2022, pp. 1–4. doi: 10.1109/ICRPSET57982.2022.10188500.
- [17] S. Younes and F. Jaouad, "Enhancement of a THz patch antenna performance using metamaterials for biomedical applications," in Proceeding of the International Conference on Connected Objects and Artificial Intelligence (COCIA2024), 2024, pp. 22–28.

5222 ISSN: 2088-8708

- doi: 10.1007/978-3-031-70411-6 4.
- [18] M. Jha, D. Samantaray, and S. Bhattacharyya, "A THz antenna with sandwiched metasurface for quadband application," Optics Communications, vol. 493, p. 126995, Aug. 2021, doi: 10.1016/j.optcom.2021.126995.
- [19] M. Hussain, W. Awan, M. Alzaidi, N. Hussain, E. Ali, and F. Falcone, "Metamaterials and their application in the performance enhancement of reconfigurable antennas: a review," *Micromachines*, vol. 14, no. 2, p. 349, Jan. 2023, doi: 10.3390/mi14020349.
- [20] W. Huang et al., "Research progress of terahertz wave dynamic control of digital coded metasurfaces," Optics and Lasers in Engineering, vol. 174, p. 107977, Mar. 2024, doi: 10.1016/j.optlaseng.2023.107977.
- [21] A. Y. I. Ashyap et al., "Triple-band metamaterial inspired antenna for future terahertz (THz) applications," Computers, Materials & Continua, vol. 72, no. 1, pp. 1071–1087, 2022, doi: 10.32604/cmc.2022.025636.
- [22] S. Younes and F. Jaouad, "Wearable patch antenna with rectangular slots and defected ground for biomedical applications," in 2023 IEEE International Conference on Contemporary Computing and Communications (InC4), 2023. doi: 10.1109/InC457730.2023.10263109.
- [23] P. Prince, G. Kaur, V. Mehta, and E. Sidhu, "Rectangular terahertz microstrip patch antenna design for vitamin K2 detection applications," in 2017 1st International Conference on Electronics, Materials Engineering and Nano-Technology, IEMENTech, 2017, pp. 1–3. doi: 10.1109/IEMENTECH.2017.8076929.
- [24] S. P. J. Christydass and N. Nurhayati, "Multiband THz rectangular microstrip patch antenna with hexagonal complementary split ring resonator," in ICRACOS 2021 2021 3rd International Conference on Research and Academic Community Services: Sustainable Innovation in Research and Community Services for Better Quality of Life towards Society 5, 2021, pp. 203–208. doi: 10.1109/ICRACOS53680.2021.9702083.
- [25] S. Younes, F. Jaouad, and K. Saidi Alaoui, "Enhancing terahertz patch antenna performance with metamaterials for biomedical applications," *TELKOMNIKA (Telecommunication Computing Electronics and Control)*, vol. 23, no. 2, pp. 267–274, 2025, doi: 10.12928/telkomnika.v23i2.26226.

BIOGRAPHIES OF AUTHORS



Kaoutar Saidi Alaoui is an assistant professor of higher education in telecommunications and electronics at the Dakhla Higher School of Technology, Ibn Zohr University, Agadir, Morocco, since 2021. She obtained her national doctorate in 2020 from the Faculty of Science and Technology in Errachidia at Moulay Ismail University in Meknes, Morocco. Currently, she is the coordinator of the electrical engineering branch at the Dakhla Higher School of Technology. Her research interests encompass optical fiber, OCDMA, and patch antennas for biomedical applications. She can be contacted at: k.alaouisaidi@uiz.ac.ma.



Younes Siraj to some contacted his master's degree in industrial computer engineering and instrumentation from the Faculty of Science and Technology Errachidia (FSTE), Moulay Ismail University, Morocco, in 2020. Presently, he is pursuing a Ph.D. at FSTE in Errachidia, Moulay Ismail University, Meknes, starting in 2022. His research focuses on the design and optimization of patch antennas for biomedical applications. He can be contacted at email: y.siraj@edu.umi.ac.ma.



Jaouad Foshi is a professor of higher education in telecommunications at the Faculty of Science and Technology in Errachidia, Morocco, since 2008. He obtained his national doctorate in 2001 from the Faculty of Sciences at Moulay Ismail University in Meknes, Morocco. Currently, he serves as the dean of FSTE. His research interests encompass the investigation of patch antennas in various applications. He can be contacted at email: j.foshi@fste.umi.ac.ma.